Fracture characteristics of new ultra-high-strength steel with yield strengths 900 – 960 MPa

P. Nevasmaa[1], P. Karjalainen-Roikonen[1], A. Laukkanen[1], T. Nykänen[2], A. Ameri[2] T. Björk[2], T. Limnell[3], J. Kuoppala[3]

[1] VTT, Technical Research Centre of Finland, Espoo, Finland
[2] Lappeenranta University of Technology, Finland
[3] Rautaruukki Oyj, Raahe, Finland

Abstract

The fracture behaviour of S960 steel in different conditions, i.e. as-delivered, cold strained, cold strained and artificially aged, has been studied using small-scale fracture mechanics and Charpy V testing as well as tests on large-scale U-beams and cold-formed rectangular hollow sections. At room temperature and -40 °C, fracture resistance testing indicated overall ductile behaviour. Regarding brittle fracture, the T0 reference temperature for the as-received material was around -50 °C. Artificial ageing alone increased this temperature only slightly, but cold-straining and artificial ageing together raised T0 (and T28J) by almost 50 °C. For the strength level studied, the FITNET correlation between T0 and T28J leads to severely un-conservative KJC estimates, indicating that KJC needs to be measured directly. T0 estimates based on fracture mechanics tests using small-scale 3-point bend specimens were clearly conservative in relation to the large-scale U-beam behaviour due to different constraints. Shear fracture occurred in the U-beam tests as a result of the small plate thickness; however, this led to only a 10 % decrease in the load-bearing capacity from the theoretical maximum load. Quasi-static bending tests on welded fatigue-cracked cold-formed rectangular hollow sections at -40 °C showed good agreement with nonlinear FEA calculations using the J-integral approach. Both large-scale test variants showed that brittle cleavage fracture will not become the dominant fracture mode in the welded beam constructions studied, provided the service temperature does not fall below -50 °C.

Keywords

ductile fracture, brittle fracture, critical crack size, ultimate capacity of cracked component, J-integral, ultra high strength steel, low ambient temperature

1. Small-scale toughness testing

Fracture behaviour was investigated using 6 mm thick ultra-high strength Optim 960 QC (S960) steel in controlled rolled & direct quenched condition. The tensile properties of the investigated S960 steel are given in Table 1.

The experimental programme comprised the following tests:

(i) standard Charpy V impact tests using sub-sized specimens (5 x 10 x 55 mm and 3 x 10 x 55 mm)
(ii) fracture mechanics tests according to ASTM E 1921 (T0 and J-R at 20 °C) using small pre-fatigued and side-grooved SE(B) specimens (5 x 10 x 55 mm^3)
(iii) fracture mechanics tests (J-R) using small pre-fatigued SE(B) specimens without side grooves (5 x 10 x 55 mm^3) at -40 °C

The following material conditions were examined:
- as-delivered parent steel: orientations LT and TL
- artificially aged (250 °C / 0.5 h) parent steel: orientation TL
- cold-strained (15 %) and artificially aged (250 °C / 0.5 h) parent steel: orientation TL
- steel from cold formed rectangular hollow section: orientation LT

Standard Charpy V tests were made to determine impact toughness transition curve, ductile-to-brittle impact toughness transition temperature T28J and the upper-shelf toughness KV_{US}. Fracture mechanics tests were conducted in accordance with ASTM E 1921 to determine the brittle fracture reference temperature T_0 (corresponding to K_{JC} = 100 MPa$\sqrt{m}$) and the fracture resistance curve for ductile fracture (i.e., J-Δ_a or J-R curve). All tests were made using sub-sized 5 x 10 x 55 mm^3 SE(B) (single edge bending) specimens, pre-fatigued with a0/W = 0.5 and side-grooved to 10 %, except J-Δa tests at -40°C without side-grooves. J-R curves were made at room temperature using partial unloading compliance.

Brittle fracture behaviour

Results of the T_0 fracture toughness tests describing the onset of brittle fracture and size-adjusted (B_0 = 25 mm) are presented in Figs. 1–4 as mean values together with 5 % and 95 % fracture probabilities.

Tensile properties of Optim 960 QC steel. *Table 1*

Condition, orientation	Rp0.2 [MPa]	Rm [MPa]	A5 [%]
As-delivered LT	1095	1182	11
As-delivered TL	1125	1215	9
Artificially aged 250 °C / 30 min TL	1222	1224	9
Rectangular hollow section, 5 mm, LT, -40 °C	1113	1210	9

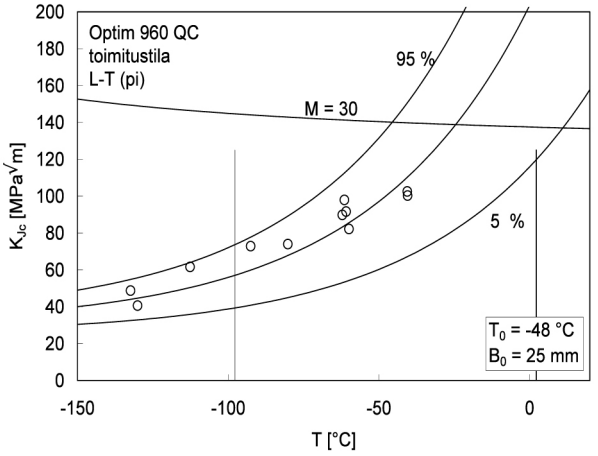

Fig. 1. Fracture toughness for as-delivered parent steel (LT) analysed acc. to ASTM E 1921. T_0 = - 48 °C. Fracture probabilities of 5, 50 and 95 % (B_0 = 25mm).

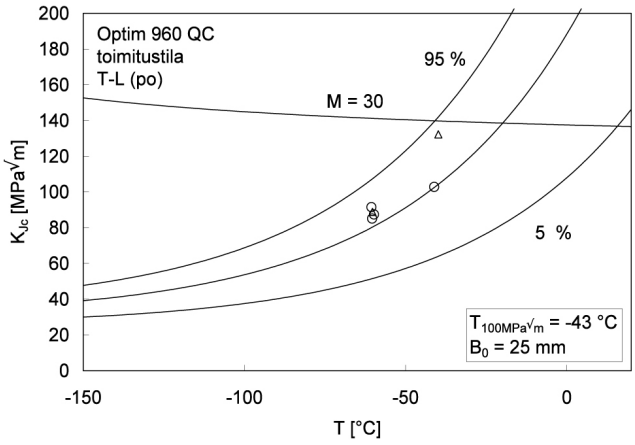

Fig. 2. Fracture toughness for as-delivered parent steel (TL) analysed acc. to ASTM E 1921. T_0 = - 43 °C. Fracture probabilities of 5, 50 and 95 % (B_0 = 25 mm).

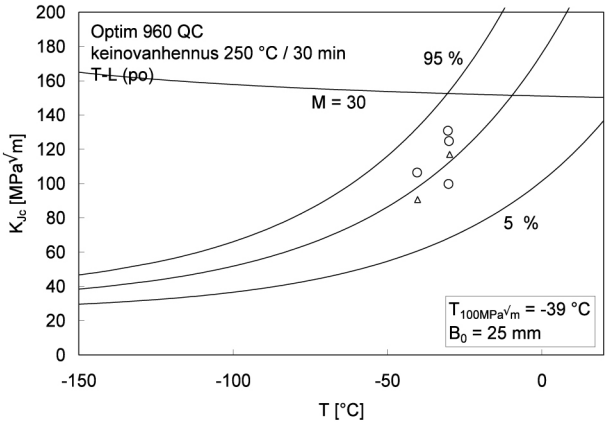

Fig. 3. Fracture toughness for artificially aged (250 °C / 0.5 h) parent steel (TL) analysed acc. to ASTM E 1921. T_0 = - 39 °C. Fracture probabilities of 5, 50 and 95 % (B_0 = 25 mm).

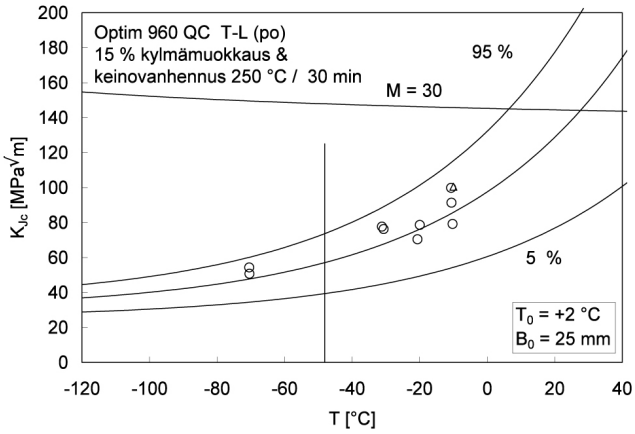

Fig. 4. Fracture toughness for cold-strained (15 %) & artificially aged (250 °C / 0.5 h) parent steel (TL) analysed acc. to ASTM E 1921 T_0 = + 2 °C. Fracture probabilities of 5, 50 and 95 % (B_0 = 25mm).

The T_0 reference temperature (K_{JC} = 100 MPa√m) measured for the as-received Optim 960 QC was around -45… -50 °C. According to Figs 1 – 4, both artificial ageing and cold-forming & artificial ageing had an adverse effect on material's fracture toughness, in relation to the as-delivered condition. In the artificially aged condition, deterioration of fracture toughness was, however, somewhat less than indicated according to the Charpy tests [1], with a shift in T_0 -temperature being only about 10 °C (T0 = -39 °C). Cold straining and artificial ageing, in turn, resulted in a significant rise of around 50 °C in both the T_0 and the T_{28J} temperatures (T_0 = +2 °C) from that in the as-delivered parent steel.

Whilst the fracture toughness test results are in line with the present knowledge [2–4] as regards the effects of cold-forming and ageing, they are in contrast with the outcome of the Charpy tests. As a result, the T0 fracture toughness temperature in relation to the T_{28J} impact toughness transition temperature no longer follows the well-known general correlation shown and validated previously [5 – 8] for ferritic steels (with the YS ranging from 250 to 1100 MPa), being:

$T_0 = T_{28J} - 18$ °C (± 1σ) , σ = ±15 °C

Consequently, estimating the fracture toughness from the Charpy data is found to lead to severely un-conservative K_{JC} estimates, see Table 2. This suggests that the correlation in its present form is not safe, as such, for ultra-high strength steel and thus, the values of K_{JC} should not be estimated for the S960 steels using only Charpy data.

Interesting to note, similar deviation from the general T_0 - T_{28J} correlation has been discovered also in a previous ECSC project [9] for conventional quenched & tempered S890 QL steel. It is therefore obvious that the

Transition temperatures T28J and T0 for the as-delivered, artificially aged and cold-strained and artificially aged Optim 960 QC steel

Table 2

Condition & orientation	T_{28J} (°C)	T_0 (°C)	$T_0 - T_{28J}$ (°C)
As-delivered ; LT As-delivered ; TL	-111 -110	-48 -43	+63 +67
Artificially aged 250 °C / 0,5 h ; TL	-72	-39	+33
Cold-strained & artificially aged 15 % & 250 °C / 0,5 h ; TL	-62	+2	+64

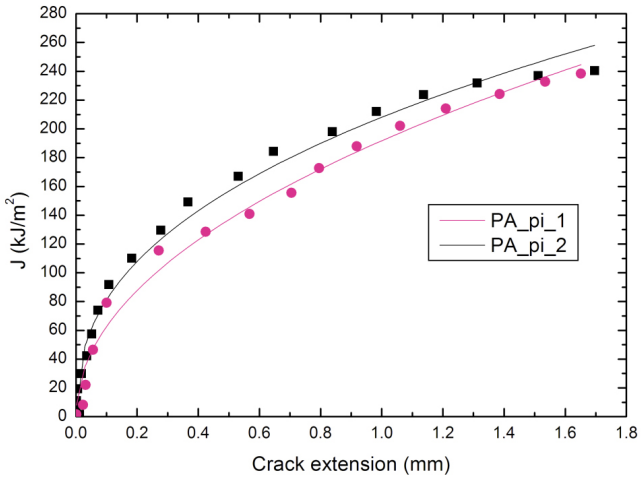

Fig. 5. Fracture resistance (J-R) curve for as-delivered parent steel (LT).

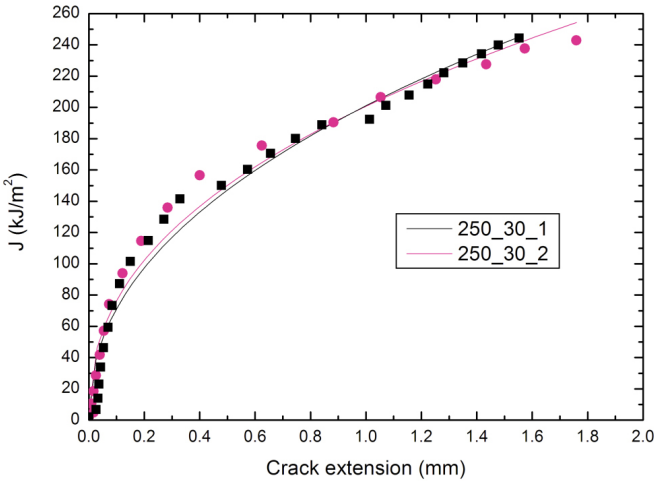

Fig. 6. Fracture resistance (J-R) curve for artificially aged (250°C/0.5 h) parent steel (TL).

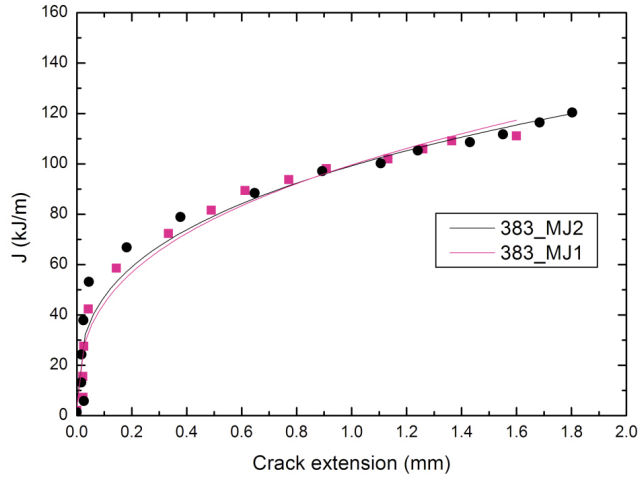

Fig. 7. Fracture resistance (J-R) curve for cold-strained (15 %) & artificially aged (250°C/0.5 h) parent steel (TL).

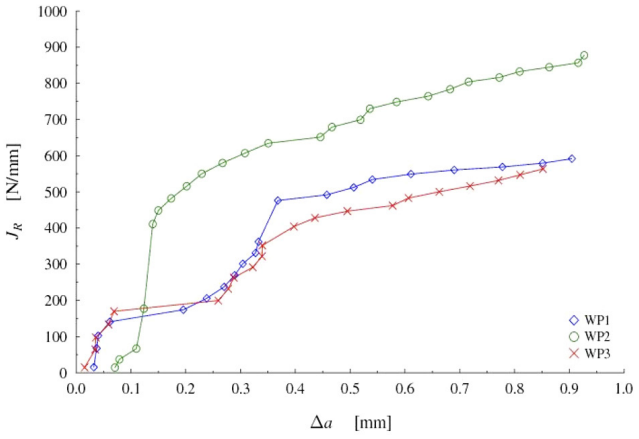

Fig. 8. Fracture resistance (J-R) curve for cold formed rectangular hollow section 5 mm (LT). Test was done without sidegrooves at -40 °C

trend for the Charpy test to overestimate the toughness behaviour in relation to the fracture toughness test is not solely a characteristic feature of the present Optim 960 QC steel, but rather a consequence of extremely high strength and the associated underlying microstructural / substructural features enabling such high strengths. It is known that both loading rate effects and notch effects are strength dependent. Thus, the fact that the deviation in the aforementioned correlation was systematically towards the same direction, i.e. the T0 temperature estimated according to the T_{28J} being un-conservative, suggests that the differences in toughness responses are related to the different natures of the quasi-static fracture toughness test (with 'sharp' pre-fatigued notch) and the dynamic Charpy test (with blunt V-notch) and that these differences become accentuated due to material's extra high strength.

- **Ductile fracture behaviour**

  The fracture resistance curves for ductile fracture (i.e., J-R -curves J-Δa) tested at room temperature are presented in Figs 5 – 7. Fig. 8 shows resistance curve for steel in cold formed condition at -40 °C.

  The J-R fracture resistance tests at RT demonstrated overall ductile fracture behaviour of the Optim 960 QC steel. Irrespective of material condition, the steel behaved in a fully ductile manner. The 'initiation' toughness (i.e. $J_{0.1mm}$ or $J_{0.2}$ mm) for the as-delivered and artificially aged condition appeared nearly equivalent, i.e. 80 – 120 kJ/m^2, whereas for the cold-strained & artificially aged condition somewhat lower values of 50–70 kJ/m^2 were recorded (Figs 5–7). The results of tests without side grooves showed much higher toughness (Fig 8). This is due to change of the loading mode during the test. Fracture surfaces of these specimens showed strong crack tunnelling and shear lip formation. Crack divided in two at surfaces in the beginning of test with low toughness. When other crack tip stopped, toughness increased.

- **Numerical evaluation of failure behaviour**

  Earlier work [10,11] have shown that in the case of thin plate, the high strength of modern structural steel can be effectively utilised as elevated design stresses without risk of brittle fracture. Due to low rigidity and restraint of thin plate structures, the welding residual stress level remains low; consequently, even at moderately low temperatures of -20…-30 °C plastic collapse tended to become the dominant failure mode of the 5–6 mm thick 650 MPa yield strength TM steel instead of brittle cleavage fracture [10,11].

  The results of FEM analyses [12] in the present study showed that static strength and fracture behaviour of the Optim 960 QC steel can be reliably and safely assessed using the 'FITNET' procedure [8] with Mis-Match Option, even in cases where local softened regions of undermatching strength exist in the welded joint area. Particularly in the case of undermatching, it is essential to apply appropriate limit load solutions for all different regions of the mis-matching weldment, in order to ensure sufficient conservatism of the FAD analysis.

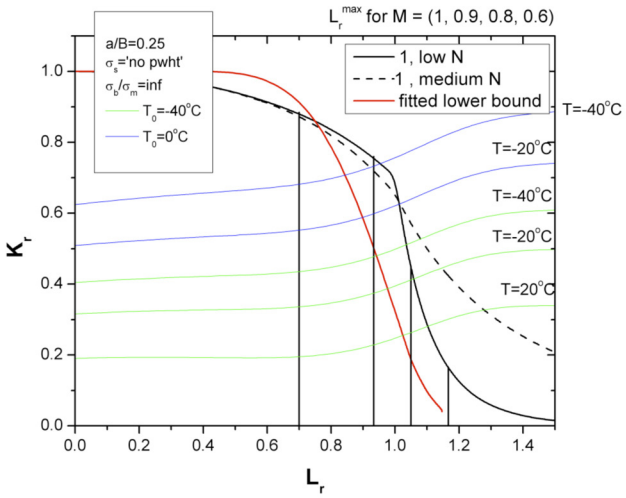

Fig. 9. Failure Assessment Diagram (FAD) for bending loaded (σ_b) 'mis-match' weldment: degree of under-matching: M, semi-elliptical surface crack (crack depth a/b = 0.25), maximum welding residual stresses assumed. Limit load solutions (L_r^{max}) made for each different degree of under-matching (M). Green lines: material's fracture toughness T_0 = -40 °C; blue lines: material's fracture toughness T_0 = 0 °C. Structure's operating temperature T = +20, -20 or -40 °C.

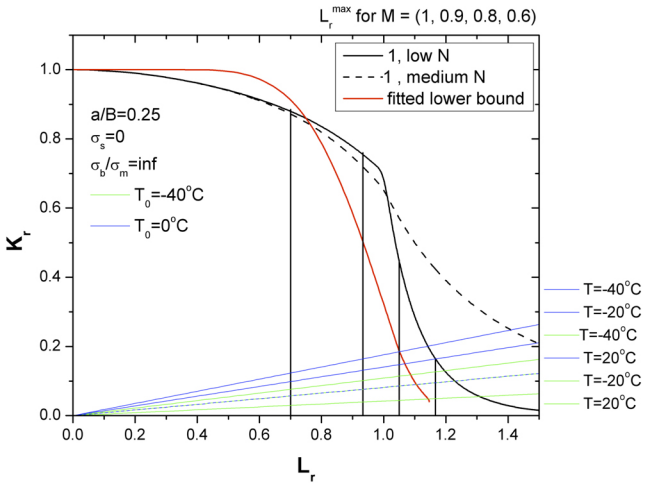

Fig. 10. Failure Assessment Diagram (FAD) for bending loaded (σ_b) 'mis-match' weldment: degree of under-matching: M, semi-elliptical surface crack (crack depth a/b = 0.25), no welding residual stresses assumed. Limit load solutions (L_r^{max}) made for each different degree of under-matching (M). : Plastic collapse dominated failure: Kr → 0 ; Lr > 1. Green lines: material's fracture toughness T_0 = -40 °C; blue lines: material's fracture toughness T_0 = 0 °C. Structure's operating temperature T = +20, -20 or -40 °C.

According to Fig. 9, conservative analysis according to the 'FITNET' procedure for the bending loaded 'mis-match' case with undermatching (M) no less than 0.6 and using postulated defect size of a/B = 0.25 (semi-elliptical surface crack) demonstrated [12], potential risk of brittle fracture can be avoided, provided the material's T0 temperature is around -40 °C and the operating temperature does not fall below -40 °C. The significant influence of welding residual stresses in the ultra-high strength material becomes apparent when comparing Figs. 9 and 10.

As shown in Fig. 11, numerical analysis according to the 'FITNET' procedure for the corresponding 'mis-match' case under tension loading demonstrate far more stringent conditions in respect to failure [12]. This accrues from the fact that pure tension load condition (where membrane stresses dominate) does not allow complete stress redistribution in a similar manner as occurs under bending loads. Assuming maximum welding residual stresses this may accentuate risk of brittle fracture, provided the material's T_0 temperature is about 0 °C (corresponding to the CGHAZ or cold-strained & artificially aged condition) and the operating temperature falls below -20 °C [12]. On the other hand, being the T_0 temperature around -40 °C (corresponding to the as-received parent steel), brittle fracture is unlikely, unless the operating temperature falls below -40 °C [12], see Fig. 11. However, even in this case structural integrity assessment according to 'FITNET' Option 2 or 3 would yield conservative (and hence safe) prediction owing to the 'cut-off' safety limits c.f. Fig. 11.

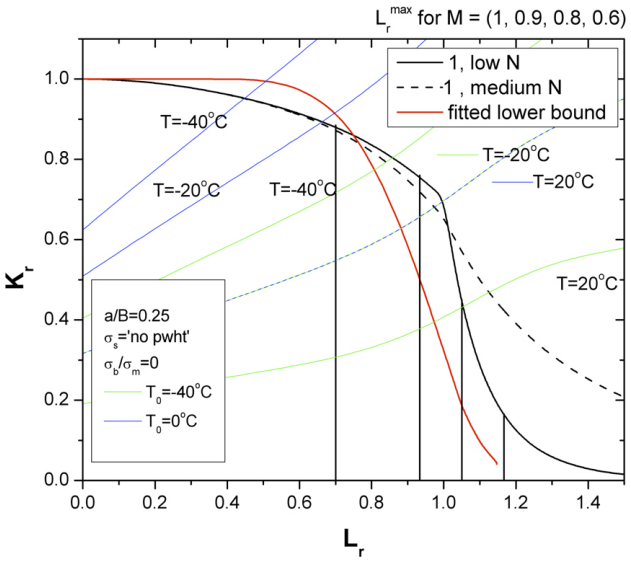

Fig. 11. Failure Assessment Diagram (FAD) for tension loaded (σ_m : membrane stress) 'mis-match' weldment: degree of under-matching: M, semi-elliptical surface crack (crack depth a/b = 0.25), maximum welding residual stresses assumed. Limit load solutions (L_r^{max}) made for each different degree of under-matching (M). Brittle fracture dominated failure: Kr → 1 ; Lr → 0. Green lines: material's fracture toughness T_0 = -40 °C; blue lines: material's fracture toughness T_0 = 0 °C. Structure's operating temperature T = +20, -20 or -40 °C.

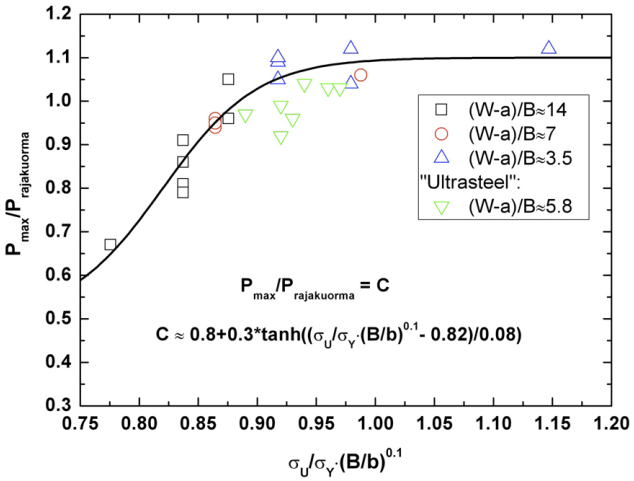

Fig. 12. Results of the large-scale U-beam tests for Optim 960 QC steel: load bearing capacity (P_{max} / $P_{limit\ load}$) as a function of a combined material strength – specimen geometry dependent parameter ($(\sigma_U / \sigma_y) * (B/b)^{0.1}$). Earlier data from "Jernkontoret" -project [5–7] as a reference.

- **2. Large-scale testing**
- **Failure behaviour in large-scale U-beam tests**

In order to verify the outcome of numerical FAD analysis and small-scale test results, it is of crucial importance to perform large-scale tests describing the 'authentic' load bearing capacity and failure behaviour of a welded structural member. In earlier works [5–7], shallow bending loaded U-profile beam specimen with a pre-fatigued notch was shown to describe realistically the appearance and effect of shear failure resulting reduction of the theoretical limit load.

Results of recorded load-displacement curves and associated fracture surface analyses of static loaded Optim 960 QC steel U-beam specimen (W x h x B x L = 100 x 90…120 x 6 x 600 mm) tests within the +20…-80 °C temperature range clearly proved [1,13] that brittle cleavage fracture does not become a dominant fracture mode until at very low temperatures of -60 °C and below. At higher temperatures in the -60…+20 °C range, the fractured surfaces revealed shear fracture propagating in the 45° orientation after initially ductile initiation [1,13]. It is noteworthy that the reduction in the limit load bearing capacity caused by the occurrence of shear fracture remained comparatively modest: all the measured maximum load values were at least 90 % of the theoretically calculated limit load, as shown in Fig. 12. Thus, with the U-beam like test specimen configuration the occurrence of shear fracture led to only a 10 %

decrease in the load-bearing capacity from the theoretical maximum load [1,13]. This, however, is obviously loading mode dependent; it should be pointed out that further experiments using 'slender' SE(B) specimens under pure bending loading indicated a somewhat greater loss of 25 %.

- **Design against brittle fracture**

Comparison between the T0 reference temperatures calculated from the fracture mechanics analysis of the U-beam test data [5–7,8,13] and those in accordance with ASTM E 1921 small-scale 5 x 10 x 55 mm3 SE(B) tests [1] revealed that the former were clearly lower than the latter. Whilst the analysis according to ASTM E 1921 gave T0 temperatures around -43…-48 ºC (see Fig. 1), those calculated from the U-beam data were in the range of -98…-107 ºC [13]. This difference can be ascribed primarily to the constraint effect (affected e.g. by the a/W -ratio) and the associated influence on the so-called T-stress parameter that, in turn, can be correlated to the Master Curve T0 temperature. The difference in T-stress between the small-scale SE(B) and large-scale U-beam specimens was roughly estimated as 100-200 MPa which translates to the T0 temperature difference of about 20–40 °C [13]. The rest of the difference is thought to originate from (i) different loading mode (i.e. pure bending in SE(B) specimens vs. combined tension and bending in U-beam specimens), (ii) difference in side-groove effects (no side-grooves in U-beam specimens vs. 10 % side-grooving in SE(B) specimens) and (iii) difference in fracture mode (shear fracture occurred only in U-beam specimens). Performing detailed elastic-plastic 3D based constraint analysis would enable more accurate quantitative description of the aforementioned differences in fracture toughness response between the applied small-scale and large-scale test specimens.

According to the experimental results, the Optim 960 QC steel studied here can effectively withstand initiation of brittle fracture in large-scale beam structures at operating temperatures commonly used for high strength steel applications. The outcome of the large-scale U-beam tests [13] and the cold-formed rectangular hollow section tests [14] was consistent in this respect; they both demonstrate that brittle cleavage fracture will not become the dominant fracture mode in the welded beam constructions studied, provided the operating temperature does not fall below -50 °C.

- **Failure behaviour in a cold-formed rectangular hollow section**

A cold-formed rectangular hollow section with dimensions W x h x B x L = 180 x 135 x 5 x 1820 mm was made from the same Optim 960 QC steel as studied in the small-scale tests. To simulate a welded structure, a single weld bead was welded around the bottom corners of the section as shown in Fig. 13a. The beam was then cyclically loaded to produce a fatigue crack that penetrated the whole bottom flange and gradually grew into the web until the critical size was reached, Fig. 13a. In one test, the crack was grown to a certain length and then the beam was subjected to a quasi-static bending load until final failure occurred. Nominal applied loads were 180 kN and 270 kN.

- **J-Integral calculation**

An elastic plastic fracture mechanics procedure (manual crack extension) was performed using a non-linear finite element method in order to define the J - a curve. That is comparable to the material resistance curve (JR - Δa) to estimate the critical crack size. The starting point for the crack simulation was at the end of the weld on the web. Fig. 14 shows the toughness required for several

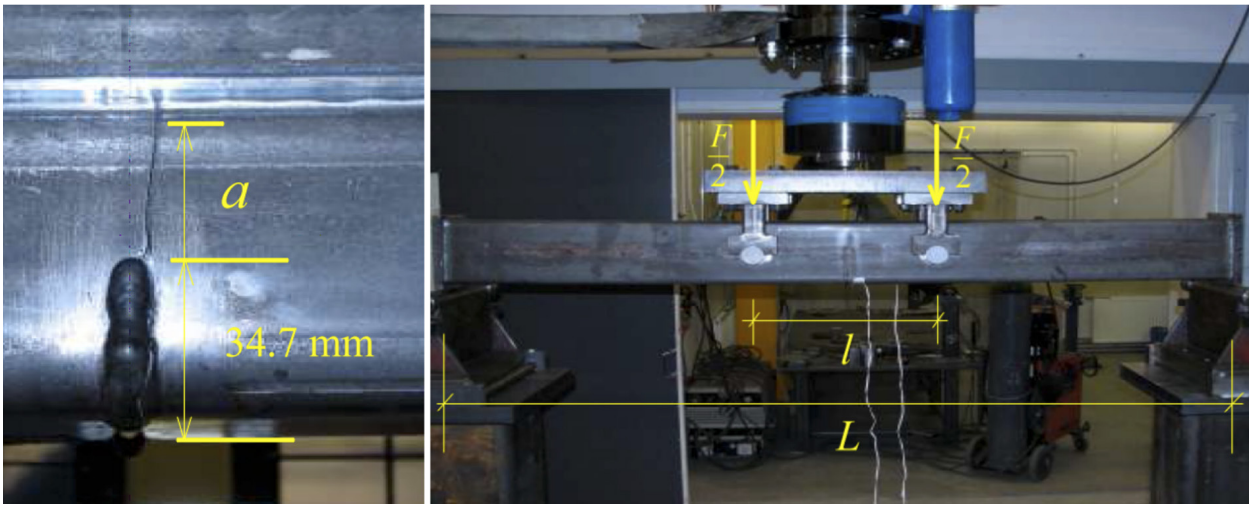

Fig. 13a & 13b. Crack starting point & Laboratory test arrangement. L = 1820 mm and l = 400 mm.

crack lengths under applied loads of 180 kN and 270 kN.

As shown in Fig. 15, the crack growth energy criterion means fracture will then occur when [15]:

$$J \geq J_R$$
$$\frac{dJ}{da} \geq \frac{dJ_R}{da} \qquad (1)$$

The critical crack size can be defined as:

$$a_c = a + \Delta a \quad \text{and} \quad a_{cr} = 34.7\ \text{mm} + a_c \qquad (2)$$
$$(a_{cr}\ \text{from outer surface of the flange})$$

where a_{cr} is the length of the symmetrical cracks in the webs of the box beam.

The critical crack size extended to outside the weld area into the parent material of the web. Consequently the resistance curve WP3 (Web Parent 3) was chosen from Fig. 8.

It was not possible to measure the real critical crack size directly from the test specimen due to the test set-up. Therefore the critical crack size was estimated by comparing the load-displacement curve with finite element analysis results obtained using several models which only differed in the size of the crack in the net section. The models which provided displacements equal to the critical displacements were taken as giving the condition of instability in the structure. The load - displacement approach based on linear elastic modelling could be used because, except for the small portion of the structure which reaches plasticity, the rest of the structure behaves elastically.

In the early stages of the crack extension, the force versus displacement curve shows a smooth drop in the magnitude of the maximum load and failure occurs when the displacement increases rapidly (Figs. 17 & 18). In the presence of a nominal load of 180 kN at - 40 oC, the critical load, F_{cr} = 160 kN and critical displacement δ_{cr} = 17.4 mm are apparent in Fig. 17. For the nominal applied load 270 kN at – 40 ºC the critical load F_{cr} = 259.6 kN and critical displacement δ_{cr}= 18.1 mm (Fig 18).

Estimation of the critical crack size according to simulated and measured beam load displacement curves are compared to calculated critical crack sizes based on elastic plastic fracture mechanics and small scale tests in Table 3.

The fracture surfaces for the tests at -40 °C were ductile and the fracture type was slanted, a combination of modes 1 and 3.

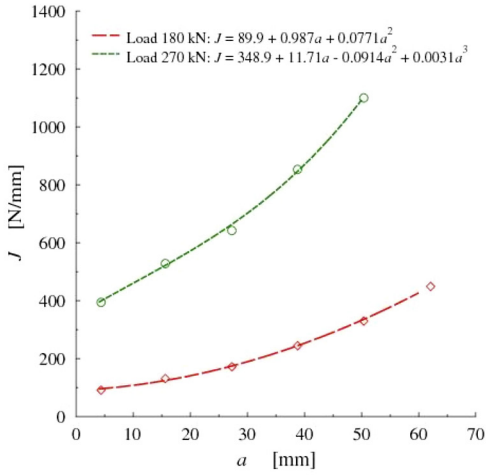

Fig.14. Calculated J – a curves.

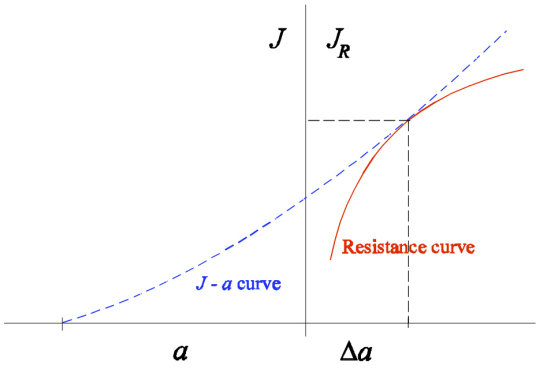

Fig. 15. Determination of critical crack length, ac.

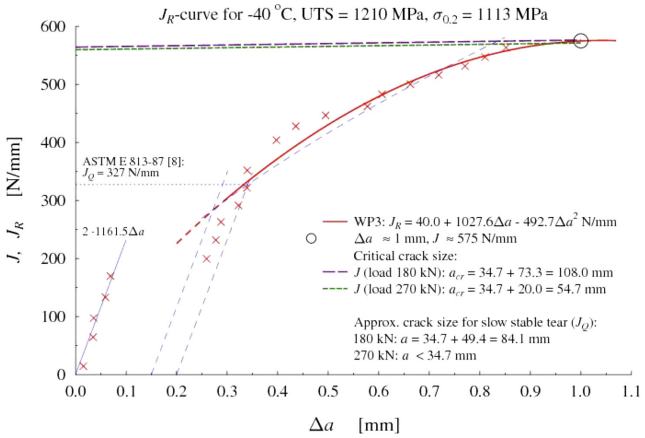

Fig. 16. Graphical solution of critical crack length, ac.

Studying the J-a curve method, reveals that the method is highly dependent on the chosen JR- curve and non-linear analysis calculation of the J integral. Estimation of the critical crack size in this method is highly dependent on the type of the fracture and the chosen resistance curve.

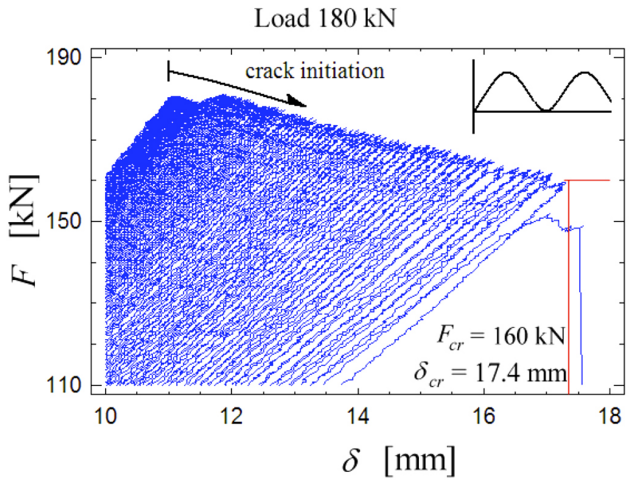

Fig. 17. Force vs. displacement behaviour of the beam under bending with nominal load 180 kN at -40 oC.

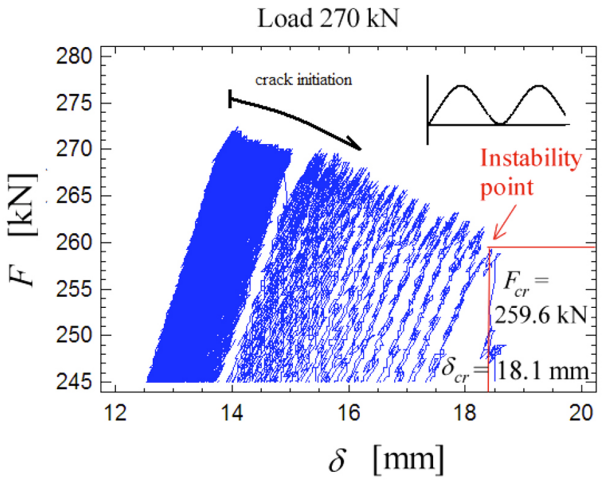

Fig. 18. Force vs. displacement behaviour of the beam under bending with nominal load 270 kN at -40 oC.

Critical crack length according to load-displacement method and elastic plastic fracture mechanics *Table 3*

			According to load displacement curve		EPFM
FNom [kN]	Fcr [kN]	t [oC]	δcr [mm]	acr [mm]	acr [mm]
180	160.0	- 40	17.4	96.6	108.0
270	259.6	- 40	18.1	62.1	54.7
210	170.0	20	19.8	96.3	

3. Conclusions

Based on the present investigation on strength and fracture characteristics of the S960 steel, the following main conclusions can be drawn:

(1) At room temperature and -40 °C, the fracture resistance (J-R) tests indicated overall ductile behaviour.

(2) Regarding brittle fracture, the T0 reference temperature (KJC = 100 MPa√m) for the as-received material was around -50 °C.

(3) Whilst the artificial ageing (250 °C / 0.5 h) increased the T0 temperature only slightly (≈ 10 °C), cold-straining (15 %) & artificial ageing in the combination resulted in nearly 50 °C increase in the T0. Similarly, the Charpy tests indicated an increase of the T28J temperature.

(4) The relation between the T0 and the T28J temperatures does not follow the general 'Fitnet' based correlation; thus, estimating the fracture toughness from Charpy data would lead to severely un-conservative KJC estimates. Consequently, KJC needs to be measured directly using fracture mechanics tests.

(5) Shear fracture occurred in the U-beam and in the rectangular hollow section tests as a result of the steel's high strength and the small plate thickness; however, this led to only a 10 % decrease in the load-bearing capacity from the theoretical maximum load according to U-beam tests.

(6) Fracture mechanical analysis revealed that the T0 estimates according to ASTM E 1921 based on fracture mechanics tests using small-scale 3-point bend SE(B) specimens were clearly conservative and hence on the safe side, in relation to the T0 estimates calculated from the large-scale U-beam test data.

(7) Both the FAD analysis according to 'Fitnet' Mis-Match Option and the outcome from the U-beam and hollow section large-scale test variants all consistently showed that brittle cleavage fracture will not become the dominant fracture mode in the welded beam constructions studied, provided the service temperature does not fall below -50 °C.

References

[1] Nevasmaa, P.; Planman, T.; Karjalainen-Roikonen, P.; Laukkanen, A. and Elers, L. 'Ultralujan suorakarkaistun ohutlevyteräksen lujuus- ja sitkeysominaisuudet'. Research Report No VTT-R-04160-08. VTT, Espoo 2008. 31 p. + Apps. (in Finnish)

[2] Porter, D., Laukkanen, A. Nevasmaa, P., Rahka, K. and Wallin, K. 'The use of TMCP steel in pressure equipment - Final report for the Finnish part of the 5th framework project ECOPRESS'. Rautaruukki Report No TR03603. Rautaruukki Oyj, Oulu 2003. 83 p

[3] Kortelainen, O., Nevasmaa, P., Wallin, K. and Porter, D. 'Effect of Cold For¬ming befo¬re Welding on HAZ Mechanical Properties and Strain Ageing Resistance in High-Strength Thermo¬mechanically Processed Steel S460ML'. Research Report No VAL B 72. VTT Manufacturing Technology, Espoo 1995. 85 p. + Apps

[4] Nevasmaa, P., Kortelainen, O., Wallin, K. and Porter, D. 'Fracture Toughness Assess¬ment and HAZ Strain Ageing Resistance of Thermomechanically Processed Steel subjected to Cold Forming before Welding'. Proc.Conf "6th International Offshore and Polar Engineering Conference (ISOPE'96)", Los Angeles, 26-31 May 1996. U.S.A: International Society of Offshore and Polar Engineers (ISOPE), 1996. Vol. IV. pp. 154–159

[5] Wallin, K. 'Methodology for selecting Charpy toughness criteria for thin high strength steels – Part 1'. Jernkontorets Forskining No D733. Jernkontoret, Stockholm 1994.

[6] Wallin, K. 'Methodology for selecting Charpy toughness criteria for thin high strength steels – Part 2'. Jernkontorets Forskining No D734. Jernkontoret, Stockholm 1994.

[7] Wallin, K. 'Methodology for selecting Charpy toughness criteria for thin high strength steels – Part 3'. Jernkontorets Forskining No D735. Jernkontoret, Stockholm 1994.

[8] FITNET Fitness-for-Service (FFS) Procedure. Vol. 1. Eds. M. Kocak, S. Webster, J.J. Janosch, R.A. Ainsworth, R. Koers. European Fitness-for-service Network. CEN 2006.

[9] Bannister, A.C, Skalidakis, M., Pariser, A., Langenberg, P., Gutierrez-Solana Salcedo, F., Sanchez, L. and Pesquera, D. 'Performance criteria for cold formed structural steels' ECSC Final Report No EUR 22056EN. Directorate General for Research, Contract No 7210-PR/246. European Commission 2006.

[10] Brederholm, A., Nevasmaa, P., Laukkanen, A., Wallin, K., Nenonen, P., Gripenberg, H., Virkkunen, I., Karppi, R. and Hänninen, H. 'Rakenteiden keventäminen termomekaanisesti valmistettuja teräksiä käyttämällä (TERMO)' Hitsaustekniikka 53(2003)2. pp. 4–13 (in Finnish)

[11] Brederholm, A., Nevasmaa, P., Laukkanen, A., Wallin, K., Nenonen, P., Gripenberg, H., Karppi, R. and Hänninen, H. 'Rakenteiden keventäminen termomekaanisesti valmistettuja teräksiä käyttämällä'. KENNO - kevyet levyt teknologiaohjelma. Teknillisen korkeakoulun Materiaalitekniikan laboratorion julkaisuja, TKK-MTR-7/02. Espoo: Teknillinen korkeakoulu, 2002. 93 p. + Apps (in Finnish)

[12] Laukkanen, A., Karjalainen-Roikonen, P., Nevasmaa, P., Andersson, T. and Elers, L. 'Fracture Mechanical Fitness-for-Purpose Assessment of Undermatching High Strength Steel Welds'. Research Report No VTT-R-01115-09. VTT, Espoo 2009. 45 p.

[13] Laukkanen, A., Nevasmaa, P., Planman, T., Karjalainen-Roikonen, P. and Elers, L. 'U-palkkikokeiden murtumismekaaninen tarkastelu'. Research Report No VTT-R-04942-09. VTT, Espoo 2009. 16 p. + Apps (in Finnish)

[14] Ameri, A. 'Calculation of the Critical Crack Size for Cold Form Rectangular Hollow Section Tube (CFRHS) under Bending Load at -40 ºC Temperature'. MScThesis. Lappeenranta University of Technology, Department of Mechanical Engineering, Laboratory of Fatigue and Strength. Lappeenranta 2009.

[15] Broek D, Elementary Engineering Fracture Mechanics, 3rd Revised Edition, Martinus Nijhoff Publishers, The Hague, The Netherlands, 1984.

For further information please contact:

Rautaruukki Corporation, Suolakivenkatu 1, FI-00810 Helsinki, Finland. Tel. +358 20 5911.
For further information please contact: info.metals@ruukki.com.